

pubs.acs.org/JPCC Article

SERS-Enabled Sensitive Detection of Plant Volatile Biomarker Methyl Salicylate

Published as part of The Journal of Physical Chemistry virtual special issue "Nanophotonics for Chemical Imaging and Spectroscopy".

Chen Song, Yongchen Wang, Yu Lei,* and Jing Zhao*



Cite This: J. Phys. Chem. C 2022, 126, 772–778



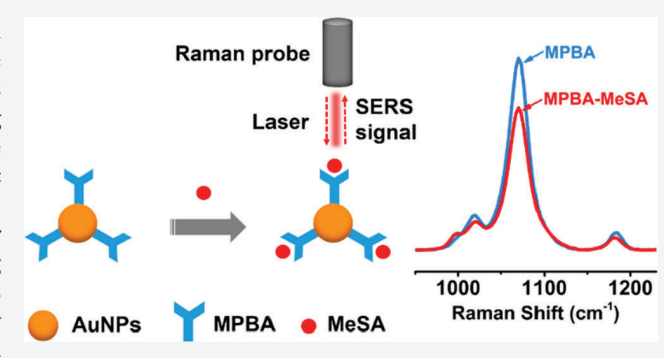
ACCESS |

Metrics & More

Article Recommendations

supporting Information

ABSTRACT: Volatile organic compounds (VOCs) contain unique information about infection of plants; thus, they can be used as reliable biomarkers for plant diseases. Among various VOCs, methyl salicylate (MeSA) is released abundantly during pathogenic infections because MeSA is emitted not only at the infected site but also throughout the whole plant as a systemic response. In this work, 4-mercaptophenylboronic acid (MPBA) functionalized Au nanoparticles were employed as a probe for MeSA vapor sensing via surface-enhanced Raman scattering (SERS) spectroscopy. The SERS sensors can detect MeSA as low as 0.608 ppb (S/N of 3) with excellent intra- and interassay reproducibility. The origin of Raman signal change was attributed



to the weak, reversible intermolecular interaction between MPBA and MeSA. This study demonstrates that the SERS sensing platform holds great promise in noninvasive and fast monitoring of volatile biomarkers for crop health.

■ INTRODUCTION

Crop losses due to pests and diseases are a major threat to the incomes of rural families and to food security worldwide. In spite of significant advances in agricultural security and crop health surveillance, crop disease outbreaks continue to pose significant concerns to agricultural industry and result in devastating economic losses. A critical step in the control and prevention of pathogen-dependent crop losses is the effective and timely detection of physiological biomarkers associated with pathogen infection, so that infections occurring on crops can be treated at an early stage before irreversible and widespread damage occurs.

Currently, the common methods for detecting pathogenic diseases in crops mainly rely on the detection of volatile organic compounds (VOCs) released by the infected plants, besides conventional time-consuming laboratory-oriented molecular diagnosis tools.³ The VOCs contain unique information about the infection and hence can be used as a reliable biomarker to rapidly and noninvasively detect pathogen infection.⁴ Unlike a healthy plant, the infected plant would release different kinds of VOCs, which were produced through various biosynthetic pathways.⁵ Among various volatile matters, methyl salicylate (MeSA) is released abundantly during pathogenic infections because MeSA is emitted not only at the infected site but also throughout the whole plant as a systemic response. Therefore, MeSA is a

suitable volatile biomarker for the detection of pathogen-associated crop diseases. MeSA is usually quantified by gaschromatography coupled with mass-spectrometry (GC-MS) and headspace solid phase microextraction (HS-SPME) techniques. However, these methods require a laboratory setting with bulky expensive instruments and skilled personnel. Thus, they are not suitable for rapid, in-field detection of MeSA. Although a few methods such as a bienzyme-based electrochemical biosensor and "electronic nose" have been developed for MeSA vapor detection, their performance still needs to be improved. 9–11

Surface-enhanced Raman spectroscopy (SERS) is a powerful technique that offers many advantages in trace analyte sensing, including high sensitivity, specificity and easiness of operation. Raman scattering of molecules refers to the inelastic scattering of photons due to their specific vibrations; therefore, can be used to identify and quantify molecules. However, the Raman signal is often weak due to low Raman scattering efficiency. Fortunately, the Raman signal can be enhanced by factors as

Received: October 22, 2021 Revised: December 6, 2021 Published: January 4, 2022





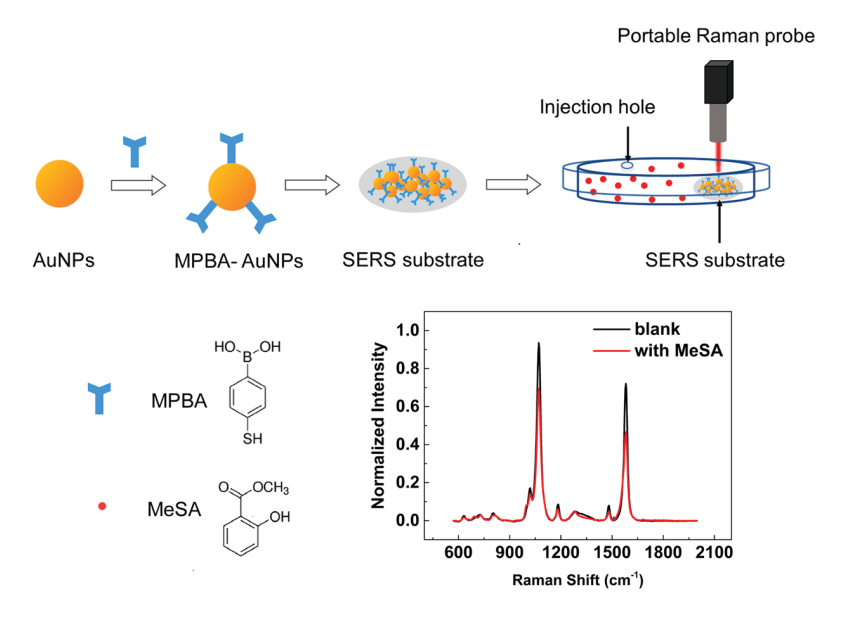


Figure 1. Generalized scheme of SERS-based detection of plant volatile biomarker methyl salicylate (not to scale). MPBA-functionalized AuNPs acted as the SERS substrate that was sealed inside a Petri dish. Various concentrations of MeSA solution were injected into the Petri dish through the hole on the Petri dish cap. The injected MeSA evaporated and interacted with MPBA on the SERS substrate, which leads to changes of the SERS signals.

high as 1015 when target molecules are on or near a metal surface with nanoscale structures, known as SERS. 12-15 The SERS enhancement is mainly due to the greatly enhanced electric field generated from localized surface plasmon resonance of the metal nanostructures. 16-18 In order to achieve high SERS intensity, it is desired that the molecules have high Raman cross-section and be close to the plasmonic structures, such as Ag and Au nanoparticles (NPs). 19-21 Some examples of the common SERS probes molecules are 4mercaptobenzoic acid,²² 4-nitrothiophenol,²³ and 4-mercaptophenol.²⁴ The SERS intensity and frequency of these probe molecules can be affected by other molecules which have chemical and/or physical interaction with them. Thus, they can be used to detect other molecules which do not have a large Raman cross section or strong interaction with the plasmonic structures. 24-28 In this work, we adopted this strategy and developed a SERS sensor for MeSA vapor detection. Specifically, 4-mercaptophenylboronic acid (MPBA) functionalized AuNPs were employed as the SERS probe. Upon exposure to MeSA vapor, the SERS signal of MPBA decreases due to the weak interaction between MPBA and MeSA. This vapor sensing method is sensitive with a limit of detection of 0.608 ppb (S/N = 3), lower than the emission level of plants. The sensor also shows good reproducibility, reusability, and specificity against some other common green leaf VOCs.

■ EXPERIMENTAL SECTION

Chemicals and Materials. 4-Mercaptophenylboronic acid (4-MPBA) was purchased from Oakwood Chemical. Methyl salicylate (MeSA), gold(III) chloride trihydrate (HAuCl₄· 3H₂O), and hydroxylamine hydrochloride were purchased from Sigma-Aldrich. Ethanol and sodium citrate dihydrate were purchased from Fisher Scientific. Hexyl acetate and *cis*-3-hexenyl acetate were purchased from Alfa Aesar. All chemicals were used as received.

Instrument. Transmission electron microscopy (TEM) images were acquired using an FEI Tecnai G2 Spirit BioTWIN and scanning electron microscopy (SEM) images were acquired with a Teneo LV SEM. A portable Raman spectrometer (QE Pro, Ocean Optics) was used to collect the Raman spectra coupled with a 785 nm laser operated at 24 mW. For each Raman measurement, the spectrum was integrated for 5 s. UV—vis spectra of AuNPs were acquired with an Agilent Technologies Cary 60 UV—vis.

Preparation of MPBA-Functionalized AuNP Films. First, 40 nm AuNPs were prepared using Frens' method²⁹ and served as the seeds for further growth. 120 nm AuNPs were then synthesized using 40 nm seeds according to our previous reported method.³⁰ UV-vis spectrum of the AuNPs suspension (Figure S1A) has a narrow peak at 591 nm, indicating that AuNPs were monodispersed. TEM imaging further confirmed AuNPs shows good size-uniformity with an average diameter of ~120 nm (Figure S1B). To functionalize the AuNPs with MPBA, 30 mL of the as-prepared AuNPs were first centrifuged and redispersed into 1 mL of DI water. Then $30 \mu L$ of a 10 mM MPBA solution (in ethanol) was added into the AuNP solution and reacted for 5 min under gentle shaking at room temperature. The excessive MPBA molecules were removed by centrifugation followed by DI water washing. This process was repeated three times to ensure the complete removal of unbounded MPBA. The MPBA-functionalized AuNPs were then dispersed into 60 μ L of ethanol. Then 5 μ L of a MPBA-AuNPs ethanolic solution was dropped onto the center of a plastic centrifuge tube cap. This process was repeated for six times after the ethanol evaporated completely each time. The MPBA-Au films were stored at room temperature and employed as the SERS substrates for MeSA

SERS Detection Method and Apparatus. The typical SERS sensing procedure developed in this study is presented in Figure 1 and briefly described below. The MPBA-Au NP substrates was placed in a Petri dish with a small injection hole in the center of Petri dish cap. Then 5 μ L of various

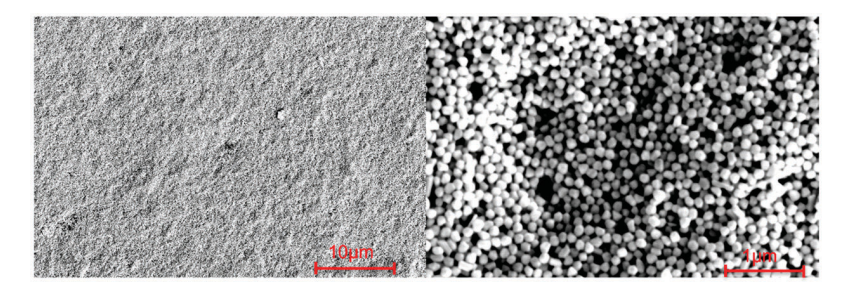


Figure 2. SEM images of the deposited MPBA-functionalized AuNPs on a plastic substrate.

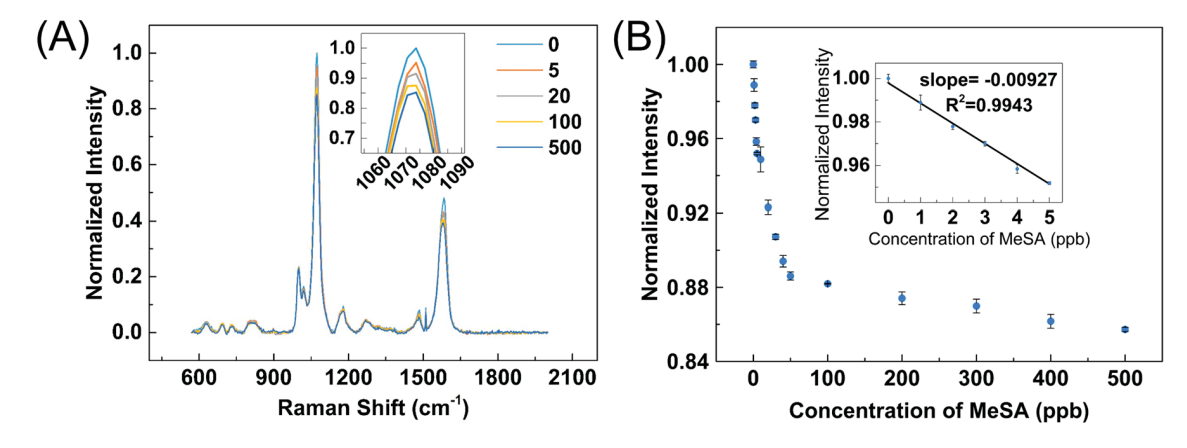


Figure 3. (A) SERS response of MPBA-functionalized AuNPs for MeSA at concentrations of 0–500 ppb. The spectra were normalized to the peak at 1074 cm $^{-1}$. Inset: a zoom-in plot of the intensity changes of the strongest peak at 1074 cm $^{-1}$. (B) MPBA detection curve by plotting the peak intensity at 1074 cm $^{-1}$ as a function of MeSA vapor concentration. Inset: a zoom-in plot of SERS intensity and MeSA concentration from 0 to 5 ppb showing a good linear relationship between the two with a R^2 of 0.9943.

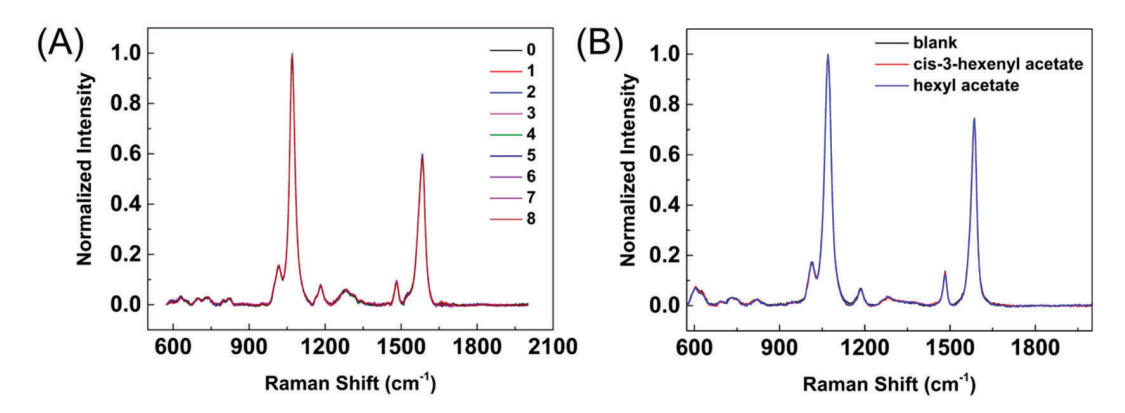


Figure 4. (A) Normalized Raman spectra upon eight injections of pure ethanol and after its vaporization. (B) Selectivity study of two representative green leaf volatiles compounds (hexyl acetate and *cis*-3-hexenyl acetate) released by plants, indicating that they have no interference during MeSA detection.

concentrations of ethanolic MeSA solutions was injected into the sealed Petri dish and then evaporated to generate MeSA vapor with different concentrations. The MeSA vapor was allowed to react with MPBA on Au NPs for 5 min. The SERS signal of MPBA on AuNPs was collected using a portable Raman spectrometer coupled with a 785 nm laser before and after MeSA addition. During detection, the positions of the portable Raman probe, the Petri dish, and the MPBA-functionalized AuNP film were all fixed.

■ RESULTS AND DISCUSSION

SEM images in Figure 2 show that MPBA-functionalized AuNPs formed a densely packed film on the substrate. Many

nanogaps formed between the AuNPs due to the aggregation during drying. These nanogaps serve as "hot spots" to enhance the Raman signal of MPBA. This procedure produces AuNP films with good uniformity of SERS signal within each film and also between different films (see results below). The SERS spectra of AuNPs before and after MPBA-functionalization were collected and shown in Figure S3. It is obvious that MPBA-functionalized AuNPs exhibit several strong SERS peaks of MPBA. The assignment of these peaks is available in Table S1. The SERS spectrum of MPBA was used as the reference for MeSA detection.

As MeSA has very low solubility in water, MeSA was dissolved into ethanol and then injected into the sealed Petri

dish to generate MeSA vapor. Then 5 μL of various concentrations of MeSA solutions was injected each time, as described in the Experimental Section. After 5 min of reaction, the SERS spectra of MPBA were collected and compared to the reference spectrum taken before MeSA addition. Assuming that after evaporation MeSA vapor uniformly filled the entire Petri dish, the vapor concentration of MeSA in the Petri dish is determined by the mass of the MeSA divided by the volume of the Petri dish. The normalized SERS intensity of MPBA shows clear dependence on MeSA concentration, as presented in Figure 3A. With the increase of MeSA concentration, the MPBA SERS signal decreases. The Raman peak intensity at 1074 cm⁻¹ was used to calculate the corresponding calibration curve (normalized peak intensity vs MeSA vapor concentration), shown in Figure 3B. The normalization is based on the SERS spectrum without MeSA (zero concentration) and the error bars represent the standard deviation calculated from three repeated measurements. The inset in Figure 3B shows the SERS sensor has a good linearity in the low ppb range. The detection limit of the sensor is determined to be 0.608 ppb using 3 times the standard deviation of the SERS measurements (0.00188) divided by absolute value of the slope of the inset linear plot (0.00927) in Figure 3B. The results demonstrate that the SERS sensor has a MeSA detectability range within the range of MeSA levels generated by plants (2.5 ppb) in studies demonstrating plant-plant MeSA signaling;³¹ thus, it can potentially be applied to directly detect MeSA vapor from plants.

Since MeSA was dissolved in ethanol, the effect of vaporized ethanol on the Raman signal of MPBA-functionalized AuNPs must be determined. The control experiments were performed following the exact same procedure of MeSA addition except that pure ethanol was used instead of MeSA in ethanol. As shown in Figure 4A, ethanol vapor generated from eight consecutive injections of 5 μ L of ethanol does not lead to observable changes of the Raman signal of MPBA-functionalized AuNPs, proving that ethanol did not interfere with the SERS detection of MeSA.

Selectivity is one important analytical characteristic for any sensors, which should be evaluated before any practical application. It has been reported that MeSA is not the only volatile organic compound produced by crops. Other VOCs such as green leaf volatiles (GLVs) that are released by plants may also be present at high concentrations, which could cause interference during MeSA measurement.^{32,33} Therefore, the selectivity study was conducted to address this query. Two representative GLVs compounds (hexyl acetate and cis-3hexenyl acetate) were used to evaluate the interference on the detection of MeSA through SERS. The experiments followed a similar procedure of MeSA detection. Specifically, 5 μ L of pure hexyl acetate and cis-3-hexenyl acetate solution were separately injected into the Petri dish. After vaporization and reaction for 5 min, SERS signals of MPBA on Au NPs were measured. From Figure 4B, there is no observable change of the SERS intensity, indicating that hexyl acetate and cis-3-hexenyl acetate did not interfere with MeSA detection.

Furthermore, another selectivity study focusing on the VOCs matrix effect (all VOCs vapors emitted from a health plant leave) on spiked MeSA detection was carried out using a real green leaf. To simulate the MeSA-releasing green leaf, a healthy green leaf was sealed in a Petri dish and then 5 μ L of MeSA was injected into it, which gave a vapor concentration of 100 ppb. After incubating for 5 min, SERS signal from MPBA-

functionalized AuNPs was measured. As shown in Figure 5, the VOCs from the green leaf did not change the MPBA SERS

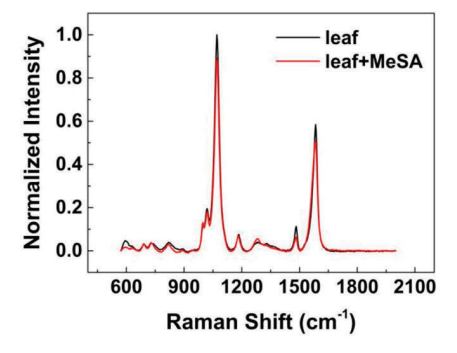
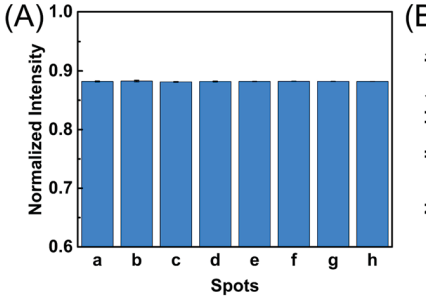


Figure 5. SERS response to MeSA with a green leaf sealed inside the Petri dish. A green leaf was sealed inside the Petri dish along with the SERS substrate MPBA—AuNPs, and then 100 ppb MeSA was injected. The SERS signal was collected 5 min later and normalized to the peak at 1074 cm⁻¹.

intensity, but the MeSA vapor from MeSA solution spiked on the green leaf did. According to the signal and the calibration curve, the calculated recovery rate is 85%, indicating the good match between the spiked and measured concentrations. This selectivity study proves that the SERS sensor possesses high selectivity toward MeSA vapor detection and the matrix VOCs released from healthy leaves do not interfere the detection of MeSA

Since SERS enhancement is extremely sensitive to the local electric-field intensity at the detection spot, a challenge in SERS detection is the intra- and interassay reproducibility. To test the intradevice reproducibility, SERS signal of MPBA before and after 100 ppb MeSA addition were collected at eight randomly selected spots on an AuNP film immobilized in a Petri dish attached to a micrometer. The micrometer reading of each spot was recorded so the SERS intensity before and after MeSA addition can be compared for each spot. Table S2 shows the SERS intensity of MPBA at 1074 cm⁻¹ before and after MeSA addition at each spot and also the relative intensity calculated by taking the ratio of the two 1074 cm $^{-1}$ peaks. The relative intensity of the data acquired at the eight spots was also plotted in Figure 6A. The difference in the normalized intensity is small, with an average of 0.882 and a relative standard deviation of 0.04%. The results show the good intradevice reproducibility of the SERS sensor. Furthermore, the interdevice variation in the relative SERS intensity at 1074 cm⁻¹ was tested when 100 ppb MeSA was added to eight different MPBA-AuNP films. The graph in Figure 6B and data in Table S3 show the results. The average relative intensity obtained from the seven devices is 0.881 with a relative standard deviation of 2%. The small intra- and interassay variation demonstrates the robustness of this method.

In the experiments, we discovered that the SERS response of the MPBA–AuNP films to MeSA is reversible. After the film was exposed to MeSA vapor in the Petri dish, we simply removed the cap and expose the film to air. The results show that 15 min exposure to clean air can recover almost 100% of the original response, indicating the interaction of MeSA with SERS reporters is reversible in principle. Furthermore, in order to examine whether the MPBA–AuNP films has long-term stability, a freshly prepared film and one film used after more than 7 months of storage in the open air in a drawer were used



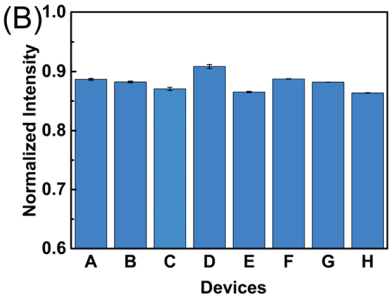


Figure 6. (A) Relative SERS intensity of MPBA at 1074 cm⁻¹ before and 10 min after 100 ppb MeSA addition, collected from eight random spots on an AuNP film, with a mean of 0.882 and RSD of 0.04%. (B) Relative SERS intensity of MPBA at 1074 cm⁻¹ before and 10 min after 100 ppb MeSA addition, collected from eight different AuNP films, with a mean of 0.881 and RSD of 2%.

for MeSA detection. After 100 ppb of MeSA was added, similar decrease (\sim 10%) in the SERS intensity of MPBA at 1074 cm $^{-1}$ was still observed as shown in Figure S4, indicating the excellent long-term stability and effectiveness of the substrate for MeSA detection. This study demonstrates that the SERS probe responds to MeSA vapor reversibly, allowing easy regeneration of SERS probe (for multiple uses) by simply placing it in clean air.

The above results demonstrated the successful detection of MeSA vapor with MPBA functionalized AuNP films. Moreover, the reversibility of the detection suggests the interaction between MPBA and MeSA is weak. Thus, we hypothesize that the MeSA molecules interact with MPBA via weak molecular interaction between MeSA and the boronic group on MPBA, resulting in a decrease in the SERS signal. Most likely, this interaction is due to Coulomb or van der Waals force between the molecules which will break the nearly $C_{2\nu}$ structural symmetry of the phenol group on MPBA to C_s . Upon close examination of the SERS spectra of MPBA after exposure to MeSA, a small shoulder appeared at 1575 cm⁻¹ from the asymmetric C-C stretching of the phenol group in MPBA due to the Herzberg-Teller contribution (see Figure 7).³⁴ Such a phenomenon has been observed in the literature, and it was attributed to the asymmetric binding of the analyte with MPBA.35 To examine how MeSA affected the SERS signal of MPBA, we calculated the intensity ratio between the asymmetric (1575 cm⁻¹) and symmetric C-C stretching

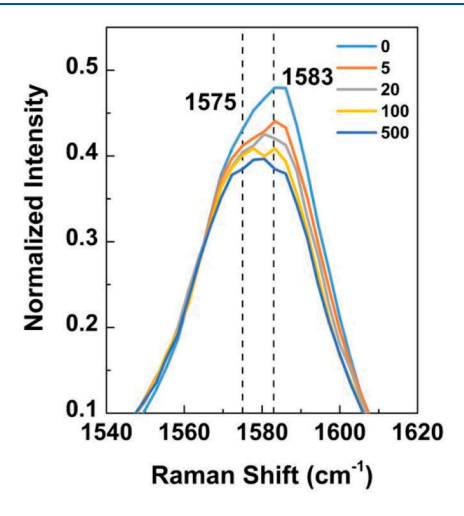


Figure 7. SERS response of MPBA-functionalized AuNPs to MeSA at different concentrations (ppb) at 1540–1610 cm⁻¹.

(1583 cm⁻¹) of the phenol group in MPBA. Figure 7 shows that as the MeSA vapor concentration increases, the ratio increases. This confirms that MeSA does interact with MPBA and breaks its symmetry. The mechanism is worthy of further investigation by varying the molecular structure of the SERS probes, and/or assistance from density functional theory calculations.

CONCLUSIONS

In this study, we have presented a rapid and facile SERS sensing platform enabled by MPBA—AuNP films using a portable Raman spectrometer. The method has successfully been applied for sensitive and selective detection of MeSA, a plant VOC released abundantly during pathogenic infections. The SERS signal of MPBA decreases upon exposure to MeSA vapor likely due to the weak binding between MeSA and boronic acid on MPBA. The SERS sensor also shows great robustness, reusability, and long-term stability, and thus, it can be applied in fast monitoring of volatile biomarkers for crop health

ASSOCIATED CONTENT

Supporting Information

The Supporting Information is available free of charge at https://pubs.acs.org/doi/10.1021/acs.jpcc.1c09185.

UV-vis spectra of Au NPs, a photo of the portable Raman probe, SERS spectra of MPBA on Au and peak assignment, and additional SERS data (PDF)

AUTHOR INFORMATION

Corresponding Authors

Jing Zhao — Department of Chemistry, University of Connecticut, Storrs, Connecticut 06269, United States; orcid.org/0000-0002-6882-2196; Phone: 860-486-2443; Email: jing.zhao@uconn.edu; Fax: 860-486-2981

Yu Lei — Department of Chemical and Biomolecular Engineering, University of Connecticut, Storrs, Connecticut 06269, United States; orcid.org/0000-0002-0184-0373; Phone: 860-486-4554; Email: yu.lei@uconn.edu; Fax: 860-486-2959

Authors

Chen Song — Department of Chemistry, University of Connecticut, Storrs, Connecticut 06269, United States

Yongchen Wang — Department of Chemistry, University of Connecticut, Storrs, Connecticut 06269, United States;

orcid.org/0000-0003-0792-2908

Complete contact information is available at: https://pubs.acs.org/10.1021/acs.jpcc.1c09185

Author Contributions

Y.L. and J.Z. conceived the project. C.S. and Y.W. synthesized and functionalized the Au NPs under J.Z. and Y.L's supervision. C.S. performed the spectroscopic measurements under J.Z. and Y.L.'s supervision. C.S., Y. L., and J.Z. analyzed the data. The manuscript was written through contributions of all authors. All authors have given approval to the final version of the manuscript.

Notes

The authors declare no competing financial interest.

ACKNOWLEDGMENTS

We thank Mr. C. H. Ji and Dr. Y. K. Huang for their help in acquiring preliminary data for the project. This work was performed in part at the Biosciences Electron Microscopy Facility of the University of Connecticut. Y.L. and J.Z. acknowledge partial financial support from NSF EECS-1916213 for developing the protocol of AuNP synthesis and functionalization.

ABBREVIATIONS

NPs, nanoparticles; MeSA, methyl salicylate; MPBA, 4-mercaptophenylboronic acid; SERS, surface-enhanced Raman scattering; VOCs, volatile organic compounds

REFERENCES

- (1) Mueller, D. S.; Wise, K. A.; Sisson, A. J.; Allen, T. W.; Bergstrom, G. C.; Bosley, D. B.; Bradley, C. A.; Broders, K. D.; Byamukama, E.; Chilvers, M. I.; et al. Corn Yield Loss Estimates Due to Diseases in the United States and Ontario, Canada from 2012 to 2015. *Plant Health Prog.* 2016, 17, 211–222.
- (2) Savary, S.; Ficke, A.; Aubertot, J.-N.; Hollier, C. Crop Losses Due to Diseases and Their Implications for Global Food Production Losses and Food Security. *Food Sec.* **2012**, *4*, 519–537.
- (3) Fang, Y.; Ramasamy, R. Current and Prospective Methods for Plant Disease Detection. *Biosensors* **2015**, *5*, 537–561.
- (4) Ponzio, C.; Gols, R.; Pieterse, C. M. J.; Dicke, M. Ecological and Phytohormonal Aspects of Plant Volatile Emission in Response to Single and Dual Infestations with Herbivores and Phytopathogens. *FunctEcol* **2013**, *27*, 587–598.
- (5) Aksenov, A. A.; Novillo, A. V. G.; Sankaran, S.; Fung, A. G.; Pasamontes, A.; Martinelli, F.; Cheung, W. H. K.; Ehsani, R.; Dandekar, A. M.; Davis, C. E. Volatile Organic Compounds (VOCs) for Noninvasive Plant Diagnostics. *ACS Symposium Series* **2013**, *1141*, 73–95.
- (6) Prithiviraj, B.; Bais, H. P.; Weir, T.; Suresh, B.; Najarro, E. H.; Dayakar, B. V.; Schweizer, H. P.; Vivanco, J. M. Down Regulation of Virulence Factors of *Pseudomonas Aeruginosa* by Salicylic Acid Attenuates Its Virulence on *Arabidopsis Thaliana* and *Caenorhabditis Elegans. Infect. Immun.* **2005**, 73, 5319–5328.
- (7) Kessler, A.; Baldwin, I. T. Defensive Function of Herbivore-Induced Plant Volatile Emissions in Nature. *Science* **2001**, *291*, 2141–2144
- (8) De Boer, J. G.; Posthumus, M. A.; Dicke, M. Identification of Volatiles That Are Used in Discrimination Between Plants Infested with Prey or Nonprey Herbivores by a Predatory Mite. *J. Chem. Ecol.* **2004**, *30*, 2215–2230.
- (9) Fang, Y.; Bullock, H.; Lee, S. A.; Sekar, N.; Eiteman, M. A.; Whitman, W. B.; Ramasamy, R. P. Detection of Methyl Salicylate Using Bi-Enzyme Electrochemical Sensor Consisting Salicylate Hydroxylase and Tyrosinase. *Biosens. Bioelectron.* **2016**, 85, 603–610.

- (10) Spinelli, F.; Noferini, M.; Vanneste, J. L.; Costa, G. Potential of the Electronic-Nose for the Diagnosis of Bacterial and Fungal Diseases in Fruit Trees. *Bull. OEPP* **2010**, *40*, 59–67.
- (11) Cui, S.; Ling, P.; Zhu, H.; Keener, H. Plant Pest Detection Using an Artificial Nose System: A Review. Sensors 2018, 18, 378.
- (12) Xu, H.; Bjerneld, E. J.; Käll, M.; Börjesson, L. Spectroscopy of Single Hemoglobin Molecules by Surface Enhanced Raman Scattering. *Phys. Rev. Lett.* **1999**, *83*, 4357–4360.
- (13) Li, K.; Stockman, M. I.; Bergman, D. J. Self-Similar Chain of Metal Nanospheres as an Efficient Nanolens. *Phys. Rev. Lett.* **2003**, *91*, 227402.
- (14) Alvarez-Puebla, R.; Liz-Marzán, L. M.; García de Abajo, F. J. Light Concentration at the Nanometer Scale. *J. Phys. Chem. Lett.* **2010**, *1*, 2428–2434.
- (15) Solís, D. M.; Taboada, J. M.; Obelleiro, F.; Liz-Marzán, L. M.; García de Abajo, F. J. Optimization of Nanoparticle-Based SERS Substrates through Large-Scale Realistic Simulations. *ACS Photonics* **2017**, *4*, 329–337.
- (16) Chen, X.; Jensen, L. Morphology Dependent Near-Field Response in Atomistic Plasmonic Nanocavities. *Nanoscale* **2018**, *10*, 11410—11417
- (17) Chulhai, D. V.; Chen, X.; Jensen, L. Simulating Ensemble-Averaged Surface-Enhanced Raman Scattering. *J. Phys. Chem. C* **2016**, 120, 20833–20842.
- (18) Zhou, Y.; Gu, Q.; Qiu, T.; He, X.; Chen, J.; Qi, R.; Huang, R.; Zheng, T.; Tian, Y. Ultrasensitive Sensing of Volatile Organic Compounds Using a Cu-Doped SnO ₂-NiO P-n Heterostructure That Shows Significant Raman Enhancement**. *Angew. Chem., Int. Ed.* **2021**, *60*, 26260.
- (19) Kleinman, S. L.; Sharma, B.; Blaber, M. G.; Henry, A.-I.; Valley, N.; Freeman, R. G.; Natan, M. J.; Schatz, G. C.; Van Duyne, R. P. Structure Enhancement Factor Relationships in Single Gold Nanoantennas by Surface-Enhanced Raman Excitation Spectroscopy. *J. Am. Chem. Soc.* **2013**, *135*, 301–308.
- (20) Wang, Y.; Yan, B.; Chen, L. SERS Tags: Novel Optical Nanoprobes for Bioanalysis. *Chem. Rev.* **2013**, *113*, 1391–1428.
- (21) Li, J.; Chen, L.; Lou, T.; Wang, Y. Highly Sensitive SERS Detection of As ³⁺ Ions in Aqueous Media Using Glutathione Functionalized Silver Nanoparticles. *ACS Appl. Mater. Interfaces* **2011**, *3*, 3936–3941.
- (22) Talley, C. E.; Jusinski, L.; Hollars, C. W.; Lane, S. M.; Huser, T. Intracellular PH Sensors Based on Surface-Enhanced Raman Scattering. *Anal. Chem.* **2004**, *76*, 7064–7068.
- (23) Xie, W.; Walkenfort, B.; Schlücker, S. Label-Free SERS Monitoring of Chemical Reactions Catalyzed by Small Gold Nanoparticles Using 3D Plasmonic Superstructures. *J. Am. Chem. Soc.* **2013**, *135*, 1657–1660.
- (24) Song, C.; Abell, J. L.; He, Y.; Hunyadi Murph, S.; Cui, Y.; Zhao, Y. Gold-Modified Silver Nanorod Arrays: Growth Dynamics and Improved SERS Properties. *J. Mater. Chem.* **2012**, *22*, 1150–1159.
- (25) Sun, F.; Galvan, D. D.; Jain, P.; Yu, Q. Multi-Functional, Thiophenol-Based Surface Chemistry for Surface-Enhanced Raman Spectroscopy. *Chem. Commun.* **2017**, *53*, 4550–4561.
- (26) Alvarez-Puebla, R. A.; Liz-Marzán, L. M. Traps and Cages for Universal SERS Detection. *Chem. Soc. Rev.* **2012**, *41*, 43–51.
- (27) Chen, Q.-Q.; Hou, R.-N.; Zhu, Y.-Z.; Wang, X.-T.; Zhang, H.; Zhang, Y.-J.; Zhang, L.; Tian, Z.-Q.; Li, J.-F. Au@ZIF-8 Core—Shell Nanoparticles as a SERS Substrate for Volatile Organic Compound Gas Detection. *Anal. Chem.* **2021**, *93*, 7188–7195.
- (28) Yang, K.; Zhu, K.; Wang, Y.; Qian, Z.; Zhang, Y.; Yang, Z.; Wang, Z.; Wu, L.; Zong, S.; Cui, Y. Ti $_3$ C $_2$ T $_x$ MXene-Loaded 3D Substrate toward On-Chip Multi-Gas Sensing with Surface-Enhanced Raman Spectroscopy (SERS) Barcode Readout. ACS Nano 2021, 15, 12996–13006.
- (29) Frens, G. Controlled Nucleation for the Regulation of the Particle Size in Monodisperse Gold Suspensions. *Nature, Phys. Sci.* 1973, 241, 20–22.

- (30) Jenkins, J. A.; Wax, T. J.; Zhao, J. Seed-Mediated Synthesis of Gold Nanoparticles of Controlled Sizes To Demonstrate the Impact of Size on Optical Properties. *J. Chem. Educ.* **2017**, *94*, 1090–1093.
- (31) Shulaev, V.; Silverman, P.; Raskin, I. Airborne Signalling by Methyl Salicylate in Plant Pathogen Resistance. *Nature* **1997**, 385, 718–721.
- (32) James, D. G. Synthetic Herbivore-Induced Plant Volatiles as Field Attractants for Beneficial Insects. *Environ. Entomol.* **2003**, 32, 977–982.
- (33) Peñuelas, J.; Llusià, J. The Complexity of Factors Driving Volatile Organic Compound Emissions by Plants. *Biol. Plant.* **2001**, 44, 481–487.
- (34) Lombardi, J. R.; Birke, R. L.; Lu, T.; Xu, J. Charge-transfer Theory of Surface Enhanced Raman Spectroscopy: Herzberg—Teller Contributions. *J. Chem. Phys.* **1986**, *84*, 4174—4180.
- (35) Sun, F.; Bai, T.; Zhang, L.; Ella-Menye, J.-R.; Liu, S.; Nowinski, A. K.; Jiang, S.; Yu, Q. Sensitive and Fast Detection of Fructose in Complex Media via Symmetry Breaking and Signal Amplification Using Surface-Enhanced Raman Spectroscopy. *Anal. Chem.* **2014**, *86*, 2387–2394.

□ Recommended by ACS

Rapid Detection of SARS-CoV-2 RNA in Human Nasopharyngeal Specimens Using Surface-Enhanced Raman Spectroscopy and Deep Learning Algorithms

Yanjun Yang, Yiping Zhao, et al. DECEMBER 23, 2022

ACS SENSORS

READ 🗹

Mapping Molecular Signatures in Plant Leaves, Flowers, and Fruits by a TiO₂ Nanotube-Based Plasmonic Chip for Imprint Mass Spectrometry Imaging

Dong Chen, Xinzhou Wu, et al.

NOVEMBER 21, 2022

ACS AGRICULTURAL SCIENCE & TECHNOLOGY

READ 🗹

In Situ Spatiotemporal SERS Measurements and Multivariate Analysis of Virally Infected Bacterial Biofilms Using Nanolaminated Plasmonic Crystals

Aditya Garg, Wei Zhou, et al.

MARCH 09, 2023

ACS SENSORS

READ 🗹

Solution-Based Ultra-Sensitive Surface-Enhanced Raman Scattering Detection of the Toxin Bacterial Biomarker Pyocyanin in Biological Fluids Using Sharp-Branched Go...

Supriya Atta and Tuan Vo-Dinh

JANUARY 24, 2023

ANALYTICAL CHEMISTRY

READ